



# Transient analysis of oxygen storage capacity of Pt/CeO<sub>2</sub>–ZrO<sub>2</sub> materials with millisecond- and second-time resolution

Evgenii V. Kondratenko<sup>a,\*</sup>, Yoshiyuki Sakamoto<sup>b,\*</sup>, Kohei Okumura<sup>b</sup>, Hirofumi Shinjoh<sup>b</sup>

<sup>a</sup> Leibniz Institute for Catalysis at University Rostock, Branch Berlin, Richard-Willstätter-Str. 12, D-12489 Berlin, Germany

<sup>b</sup> Toyota Central R&D Labs., Nagakute-cho, Aichi-gun, Aichi-ken, 41-1 Aza Yokomichi, Oaza Nagakute 480-1192, Japan

## ARTICLE INFO

### Article history:

Received 12 November 2008

Received in revised form 12 January 2009

Accepted 14 January 2009

Available online 23 January 2009

### Keywords:

Oxygen storage capacity

Mechanism

TAP

Platinum

Ceria

## ABSTRACT

A simple method for determining the speed of oxygen release from Pt/CeO<sub>2</sub>–ZrO<sub>2</sub> materials is proposed. We determined the speed of oxygen release from three differently prepared Pt(1 wt%)/CeO–ZrO<sub>2</sub> catalysts by two methods: the method employing temporal analysis of products (TAP) reactor with CO, O<sub>2</sub>, and CO<sub>2</sub> pulsed gases, and a conventional method with CO and O<sub>2</sub> switch gases. Strong CO<sub>2</sub> adsorption precluded correct analysis of oxygen release speed, when it was determined from the amount of CO<sub>2</sub> formed. Therefore, instead of the amount of CO<sub>2</sub> formed, we suggested the  $t_{\max}$  value, defined as the position of maximal intensity of CO<sub>2</sub> transient responses obtained upon low-intensity ( $10^{15}$ – $10^{16}$  molecules) CO pulsing in the TAP reactor. Shorter the  $t_{\max}$  value, higher the rate of oxygen release, because the temperature dependence of the  $t_{\max}$  determined in the present study resembles the previous results of oxygen release analysis [T. Tanabe, A. Suda, C. Descorme, D. Duprez, H. Shinjoh, M. Sugiura, Stud. Surf. Sci. Catal. 138 (2001) 135].

© 2009 Elsevier B.V. All rights reserved.

## 1. Introduction

Three-way (TW) catalysts are widely used for cleaning automotive exhaust gases. A key feature of these catalysts is their oxygen storage capacity (OSC), ensuring that the air-to-fuel ratio is maintained at ca. 14.6 between the lean-rich cycles. This is an important requirement for the effective removal of HC, CO, and NO<sub>x</sub> [1,2]. In general, OSC is defined as the amount of oxygen stored by catalytic materials and can be supplied for oxidative reactions. It is well known that CeO<sub>2</sub>-based materials possess high OSC [3–11]. There are three classical methods for determining OSC: (i) temperature-programmed reduction using CO or H<sub>2</sub> as reducing agents, (ii) CO or H<sub>2</sub> pulse experiments with time resolution in seconds, and (iii) oxygen chemisorption at room temperature after catalyst reduction by hydrogen at high temperatures. However, the conditions employed in these methods may greatly influence the measured OSC values, and consequently affect their possible relationship with the catalytic performance under the operating conditions of automotive TW catalysts. Several years ago, Sakamoto et al. [12] have suggested a new method for determining OSC performance by measuring the amount of oxygen storage/

release from planar catalysts on the millisecond scale using two CO pulses with millisecond pulse width. They concluded that the speed of oxygen release rather than the overall OSC values is an essential property of active OSC catalysts. Tanabe et al. [9] have evaluated the oxygen release speed from the initial amount of CO<sub>2</sub> formed upon switching from O<sub>2</sub> to CO. Their results agree well with the CO conversion at 473 K under conditions simulating the performance of a real automotive engine. Therefore, it is very important to correctly determine the OSC and oxygen release speed. However, these characteristics alone do not provide any fundamental insights for rational catalyst design. We believe that for developing more efficient automotive three-way catalytic materials, it is essential to establish the basic relationships between the OSC reaction mechanism and the physico-chemical properties of solids, such as dispersion of precious metals, surface area, grain size, and crystal structure of OSC materials.

Based on the above background, the present contribution focuses on elucidating mechanistic details of primary and secondary reaction pathways in oxygen-free CO oxidation to CO<sub>2</sub>, and discovers the relationship between catalytic performance of solid materials in this reaction and their composition. For this purpose, the temporal analysis of products (TAP) reactor operating with sub-millisecond-time resolution along with conventional CO and O<sub>2</sub> switch experiments with second-time resolution were applied to investigate selective (CO<sub>2</sub> formation) and non-selective (CO<sub>2</sub> adsorption/desorption) routes of CO oxidation over three

\* Corresponding authors.

E-mail addresses: [evgenii.kondratenko@catalysis.de](mailto:evgenii.kondratenko@catalysis.de) (E.V. Kondratenko), [sakamoto@mosk.tytlabs.co.jp](mailto:sakamoto@mosk.tytlabs.co.jp) (Y. Sakamoto).

**Table 1**Physico-chemical properties of Pt/CeO<sub>2</sub>–ZrO<sub>2</sub> materials.

Physico-chemical properties	Catalysts		
	Pt/CZ-D	Pt/CZ-O	Pt/CZ-R
Pt loading/wt%	1	1	1
Ce/Zr ratio	1	1	1
XRD structure	Cubic (Ce <sub>0.5</sub> Zr <sub>0.5</sub> O <sub>2</sub> )	Cubic (CeO <sub>2</sub> ), tetragonal (ZrO <sub>2</sub> )	κCe <sub>0.5</sub> Zr <sub>0.5</sub> O <sub>2</sub>
S <sub>BET</sub> /m <sup>2</sup> g	58	129	3
Pt dispersion/%	59	23	2
Pt surface density/Pt nm <sup>−1</sup>	0.53	0.24	10.3
Oxide grain size	20	10	200

Pt(1 wt%)/CeO<sub>2</sub>–ZrO<sub>2</sub> catalysts. These materials have been previously characterized [9,13] by various physico-chemical methods (BET, oxygen isotopic exchange, and XRD). The most relevant characterization results are summarized in Table 1. Three main factors governing the OSC performance of these catalytic materials are: (i) specific surface area of CeO<sub>2</sub>–ZrO<sub>2</sub>, (ii) dispersion of Pt and (iii) homogeneous distribution of Zr in CeO<sub>2</sub>. According to [13], cubic CeO<sub>2</sub> and tetragonal ZrO<sub>2</sub> phases coexist in Pt/CZ-O, while Pt/CZ-D is a solid solution of Ce<sub>0.5</sub>Zr<sub>0.5</sub>O<sub>2</sub>. A κCe<sub>0.5</sub>Zr<sub>0.5</sub>O<sub>2</sub> phase was identified in Pt/CZ-R, where Zr ions are distributed homogeneously in the lattice of CeO<sub>2</sub>. In order to identify common factors influencing the OSC performance, mechanistic insights into CO oxidation and CO<sub>2</sub> adsorption/desorption are related to the above physico-chemical properties of these Pt(1 wt%)/CeO<sub>2</sub>–ZrO<sub>2</sub> catalysts.

## 2. Experimental

### 2.1. CO and O<sub>2</sub> transient experiments at ambient pressure

Transient ambient-pressure analysis of the reduction of Pt/CZ-O, Pt/CZ-D, and Pt/CZ-R materials by CO and their reoxidation by O<sub>2</sub> was performed in an in-house-developed setup equipped with two 4-port valves. These valves enable switching between different reaction feeds, avoiding any contact between the feeds. A tubular fixed-bed quartz reactor (internal diameter 6 mm) was employed for the catalytic tests. The temperature within the catalyst particles bed was measured using an axially movable thermocouple located inside the quartz capillary. The catalyst quantity was fixed as 320 mg. The catalyst sample (sieve fraction 250–350 μm) was packed within the isothermal zone of the quartz reactor between two layers of quartz particles of the same sieve fraction. Before transient experiments with a CO-containing feed (CO/Ar/Ne = 10/10/40, 60 ml<sub>(STP)</sub> min<sup>−1</sup>) were performed, the catalysts were heated in an O<sub>2</sub> flow (O<sub>2</sub>/Ne = 10/40, 50 ml<sub>(STP)</sub> min<sup>−1</sup>) up to 523 K with a heating rate of 10 K min<sup>−1</sup> at ambient pressure for 30 min. Thereafter, transient experiments were performed in the temperature range of 523–623 K, starting at 523 K with a temperature step of 50 K. Additionally, before transient experiments at 573 and 623 K were carried out, the catalysts were reoxidized in an O<sub>2</sub> (O<sub>2</sub>/Ne = 10/40) flow at these respective temperatures for 30 min. The duration of the CO and O<sub>2</sub> cycles at each temperature was 20 min. In order to avoid co-feeding of O<sub>2</sub>- and CO-containing mixtures, the catalysts were flushed with pure Ne for 5 min between the O<sub>2</sub> and CO cycles.

A quadrupole mass spectrometer (Baltzer Omni Star 200) was used for quantitative analysis of reactants and reaction products. Transient responses at the reactor outlet were monitored at the following atomic mass units (AMU): 44 (CO<sub>2</sub>), 40 (Ar), 32 (O<sub>2</sub>), 28 (CO<sub>2</sub>, CO), and 20 (Ne). The concentration of feed components and reaction products was determined from the respective AMUs using standard fragmentation patterns and sensitivity factors, which were determined separately in calibration experiments.

### 2.2. Transient experiments in the TAP reactor

Mechanistic analysis of CO, O<sub>2</sub>, and CO<sub>2</sub> interactions with Pt/CZ-O, Pt/CZ-D, and Pt/CZ-R was performed in the Temporal Analysis of Products (TAP-2) reactor a transient pulse technique with sub-millisecond-time resolution [14,15]. The catalyst sample (sieve fraction 250–350 μm) was packed within the isothermal zone of the homemade quartz micro-reactor (40 mm length and 6 mm internal diameter) between two layers of quartz particles of the same sieve fraction. The catalyst quantity was fixed as 10 mg. The catalyst was pretreated in vacuum (10<sup>−5</sup> Pa) at 773 K (heating rate of 10 K min<sup>−1</sup>) for 30 min followed by decreasing its temperature to 523 K in vacuum. Thereafter, transient experiments were performed in the temperature range from 523 to 623 K, starting at 523 K with a temperature step of 50 K. Before each experiment, the catalysts were oxidized by O<sub>2</sub> pulses (in total ca. 10<sup>18</sup> O<sub>2</sub> molecules).

Four different pulse experiments were conducted. The pulse size of CO in multi-pulse and sequential-pulse experiments was in the range of 10<sup>15</sup>–10<sup>16</sup> molecules, while the CO<sub>2</sub> pulse size was ca. 2 × 10<sup>14</sup> molecules.

1. The catalyst's ability for initial oxygen storage was determined by means of CO multi-pulse experiments, in which a mixture of CO and Ne (CO/Ne = 1/1) was repeatedly pulsed over the O<sub>2</sub>-pretreated catalyst.
2. The reactivity of adsorbed oxygen species for CO oxidation was investigated by sequential pulsing of O<sub>2</sub>/Xe = 1/1 and CO/Ne = 1/1 mixtures with a time delay (Δt) of 0.1 s between the pulses.
3. In order to analyze whether CO or CO-containing species may be stored on the catalyst and oxidized by O<sub>2</sub>, CO/Ne = 1/1 and O<sub>2</sub>/Xe = 1/1 mixtures were sequentially pulsed with Δt = 0.1 s.
4. CO<sub>2</sub>/Ne = 1/1 pulse experiments were performed over oxidized catalysts in order to investigate adsorption/desorption behavior of CO<sub>2</sub>.

A quadrupole mass spectrometer (HAL RC 301 Hiden Analytical) was used for quantitative analysis of reactants and products. The transient responses at the reactor outlet were monitored at the following atomic mass units (AMU): 132 (Xe), 44 (CO<sub>2</sub>), 32 (O<sub>2</sub>), 28 (CO<sub>2</sub>, CO), and 20 (Ne). The concentrations of feed components and reaction products were determined from the respective AMUs using standard fragmentation patterns and sensitivity factors according to the following procedure.

The relative sensitivities (*A<sub>i</sub><sup>r</sup>*) of feed components and reaction products were determined as the ratio of the areas under the response signals of each compound to the area under the response signal of the inert gas (Ne or Xe). The respective areas were corrected according to the contribution of fragmentation pattern of different compounds to the measured AMU signal. The mole fractions *κ<sub>i</sub>* of gas-phase components were calculated according to Eq. (1). Calculation of conversion *X<sub>i</sub>* and yield *Y<sub>i</sub>* was performed using Eqs. (2) and (3), respectively:

$$\kappa_i = \frac{\kappa_{\text{inert}}^0 \cdot A_{\text{exp},i}^r}{A_{\text{cal},i}^r} \quad (1)$$

$$X_i = \frac{A_{\text{cal},i}^r - A_{\text{exp},i}^r}{A_{\text{cal},i}^r} \quad (2)$$

$$Y_i = \frac{v_{\text{educt}} \cdot \kappa_{\text{product},i}^{\text{out}}}{v_{\text{product},i} \cdot (\kappa_{\text{educt}}^0)} \quad (3)$$

where *A<sub>exp,i</sub><sup>r</sup>* is the relative sensitivity observed over each catalyst, *A<sub>cal,i</sub><sup>r</sup>* is the relative sensitivity determined separately for the same reactant mixture in the reactor filled with inert material, *κ<sub>inert</sub><sup>0</sup>* is

the molar fraction of the inert gas in this mixture,  $\kappa_{educt}^0$  is the molar fraction of feed component at the reactor inlet,  $\kappa_{product,i}^{out}$  is the molar fraction of the product at the reactor outlet,  $\nu_{educt}$  and  $\nu_{product,i}$  are stoichiometric coefficients of feed components and reaction products, respectively.

### 3. Results and discussion

#### 3.1. CO and O<sub>2</sub> cyclic experiments at ambient pressure

Fig. 1 exemplifies transient responses of O<sub>2</sub>, CO, and CO<sub>2</sub> recorded upon alternating feeding of CO/Ar/Ne = 10/10/40 and O<sub>2</sub>/Ne = 10/40 mixtures over Pt/CZ-D, Pt/CZ-O, and Pt/CZ-R at 523 K. The responses were height normalized for better comparison of their shapes. One can see that CO<sub>2</sub> was formed over Pt/CZ-R only in

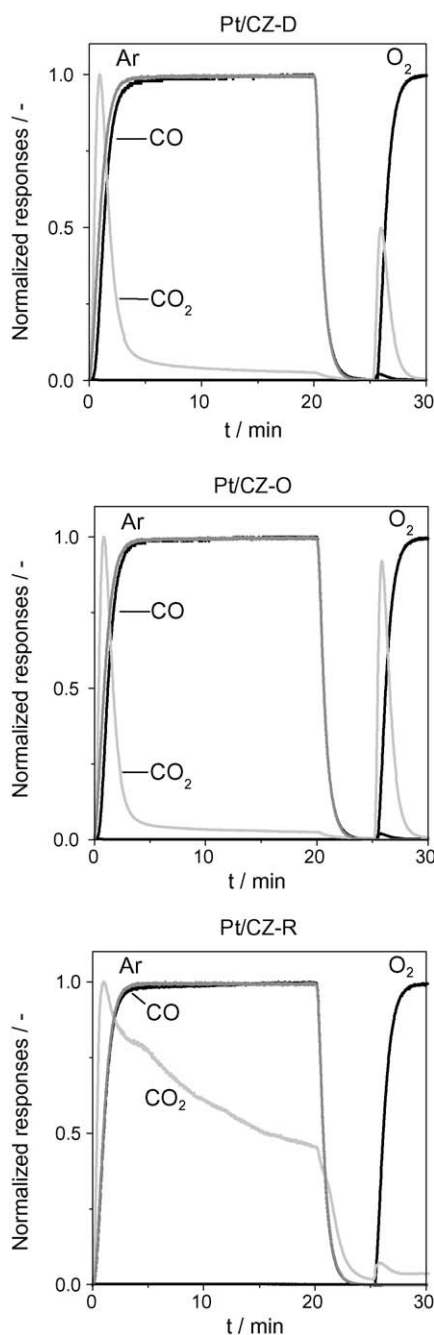


Fig. 1. Transient profiles of CO, O<sub>2</sub>, and CO<sub>2</sub> during reduction and reoxidation of Pt/CZ-D, Pt/CZ-O, and Pt/CZ-R by CO and O<sub>2</sub> at 523 K, respectively.

the CO period, while CO<sub>2</sub> was observed over Pt/CZ-D and Pt/CZ-O in both the O<sub>2</sub> and CO periods. Similar results were also obtained at other reaction temperatures. Since gas-phase O<sub>2</sub> was not present in the CO period, the formation of CO<sub>2</sub> indicates that the catalysts possess oxygen species, which are able to oxidize CO to CO<sub>2</sub> and are easily removed from the solid materials. This conclusion is in agreement with several previous studies on CO oxidation over various Ce-based catalytic materials [16–19]. In contrast to these earlier studies, our present results demonstrate that CO<sub>2</sub> production is strongly influenced by the distribution of Pt and by the morphology of CeO<sub>2</sub>–ZrO<sub>2</sub> materials possessing the same ratio of Zr/Ce. The formation of CO<sub>2</sub> over Pt/CZ-O and Pt/CZ-D in the O<sub>2</sub> period can be due to the fact that CO from the CO period was stored on the catalyst surface as a carbonate intermediate as experimentally shown in [16,17,20] for Ce<sub>x</sub>ZrO<sub>1-x</sub>O<sub>2</sub> materials ( $0.15 \leq x \leq 1$ ).

It is also important to note that the production of CO<sub>2</sub> over Pt/CZ-O and Pt/CZ-D in the CO period was observed during ca. 3 min of stream. In contrast to these catalysts, CO<sub>2</sub> is formed over Pt/CZ-R during the entire CO period, i.e., 20 min of CO stream. Moreover, the shape of the CO<sub>2</sub> transient over Pt/CZ-R is very broad compared to that over Pt/CZ-O and Pt/CZ-D. This experimental finding may indicate the presence of differently active oxygen species over Pt/CZ-R. Moreover, their reactivity depends on the reduction degree of the catalyst.

In order to quantify CO<sub>2</sub> production over the catalysts studied, the amount of CO<sub>2</sub> formed in the CO period was calculated by integrating non-normalized CO<sub>2</sub> transients. The results obtained are presented in Fig. 2. For all the catalysts, the total amount of CO<sub>2</sub> increases with an increase in reaction temperature, indicating that CO oxidation to CO<sub>2</sub> is an activated process. The most significant influence of temperature on the CO<sub>2</sub> production occurred with Pt/CZ-R, which shows a superior OSC performance at 573 and 623 K. The stronger temperature dependence of CO<sub>2</sub> formation over Pt/CZ-R compared to Pt/CZ-D and Pt/CZ-O indicates that the activation energy of CO oxidation over Pt/CZ-R is higher than over the two latter catalysts. The tendency at 523 K was similar to the CO conversion at 473 K in a cyclic transient reaction, which emulated real automotive reaction conditions, whereas the tendency at 623 K was similar in terms of the oxygen storage capacity [9], but it differed in terms of O<sub>2</sub> release speed.

Considering the amount of CO<sub>2</sub> formed in the CO period and the overall amount of CeO<sub>2</sub> in the catalysts, the CO<sub>2</sub>/Ce ratio was calculated for different temperatures (Fig. 3). The Pt/CZ-R catalyst shows the highest CO<sub>2</sub>/Ce ratio at 573 and 623 K. These results suggest that Pt/CZ-R possesses a higher concentration of easily

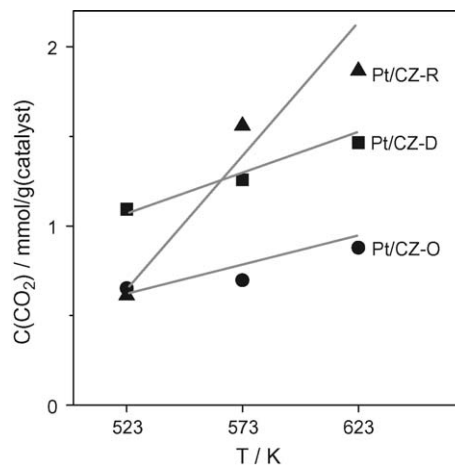
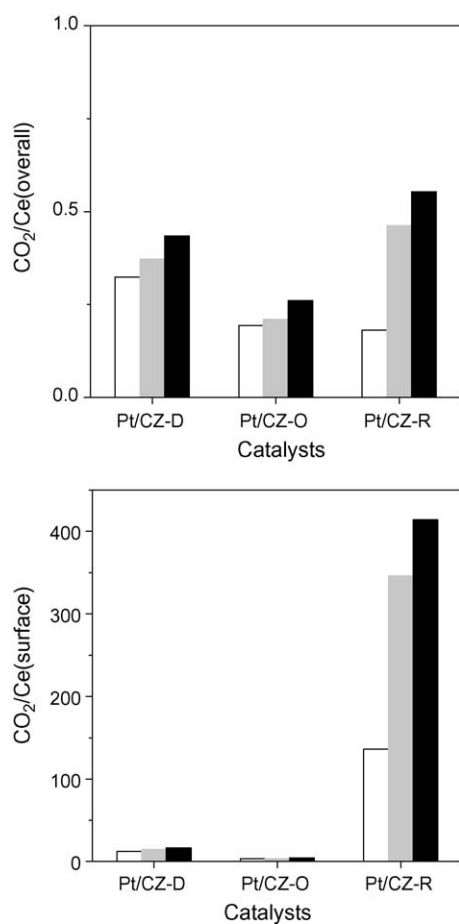


Fig. 2. Amount of CO<sub>2</sub> formed over Pt/CZ-D, Pt/CZ-O, and Pt/CZ-R in the CO period at different temperatures.



**Fig. 3.** Ratios of CO<sub>2</sub>/Ce calculated from the amount of CO<sub>2</sub> formed over Pt/CZ-D, Pt/CZ-O, and Pt/CZ-R in the CO period at different temperatures; white, gray, and black bars are for 523, 573, and 623 K, respectively.

reducible CeO<sub>x</sub> species compared to Pt/CZ-D and Pt/CZ-O. In order to investigate whether surface and/or bulk Ce<sup>4+</sup> cations participate in the redox process responsible for oxygen-free oxidation of gas-phase CO to CO<sub>2</sub>, the surface concentration of Ce species was estimated. According to [21], the number of surface oxygen atoms over Pt/CZ-D, Pt/CZ-O, and Pt/CZ-R is ca. 3 μmol m<sup>-2</sup>. For the Ce/O ratio of 0.5, the number of surface Ce atoms should be ca. 1.5 μmol m<sup>-2</sup>. Since the ratio of CO<sub>2</sub>/Ce(surface) given in Fig. 3 is greater than 1, bulk Ce atoms participate in surface redox processes. The highest ratio was determined for the Pt/CZ-R catalyst, which possesses the largest oxide grain size and the most homogeneous distribution of Zr in the CeO<sub>2</sub> lattice. When these two parameters decrease, the ability of bulk CeO<sub>x</sub> species in oxygen-free CO oxidation decreases. This result is in agreement with [13].

For further deeper mechanistic insights into the OSC chemistry, transient experiments with CO and O<sub>2</sub> were performed in the TAP reactor operating at millisecond contact times, which are similar to fluctuations under the operation conditions of automotive catalyst. The results are presented and discussed in the next section.

### 3.2. Mechanistic analysis of CO oxidation with millisecond-time resolution

Oxygen-free CO pulse experiments were performed at 523, 573, and 623 K. Since the amount of CO pulsed in these experiments was considerably lower than the total amount of oxygen, which can be removed from the catalysts, initial OSC performance is

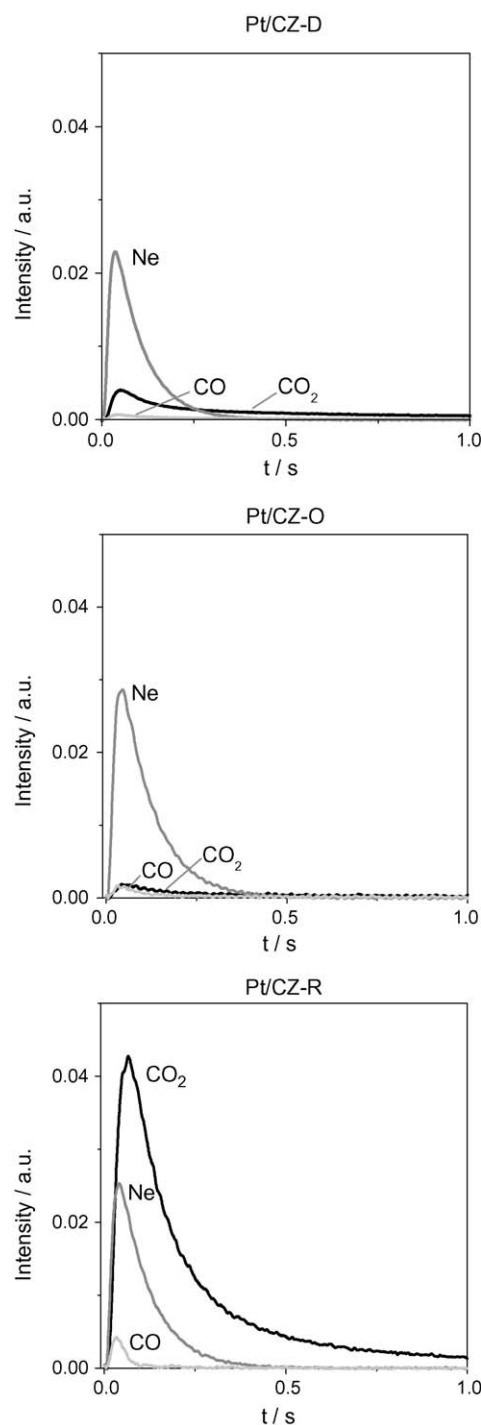


**Fig. 4.** Transient responses of CO, Ne, and CO<sub>2</sub> after CO (CO/Ne = 1/1) pulsing over Pt/CZ-D, Pt/CZ-O, and Pt/CZ-R at 623 K. Pulse size of CO is ca. 10<sup>15</sup>.

determined. For proper comparison of the catalytic performance of different materials, the sample amount was fixed as 10 mg, resulting in the height of the catalyst bed of 0.3 mm. Smaller the bed height, lesser is the possible effect of readsorption of reaction products on the reaction studied. The transient responses of Ne, CO, and CO<sub>2</sub> after CO/Ne = 1/1 pulsing over Pt/CZ-D, Pt/CZ-O, and Pt/CZ-R at 623 K are presented in Fig. 4. The degree of CO conversion approached completion over all the catalysts. The highest amount of CO<sub>2</sub> was detected over Pt/CZ-R followed by Pt/CZ-D and Pt/CZ-O. The result is in agreement with the results of transient experiments at ambient pressure in Section 3.2.

Since the low- $\text{CO}_2$  production in oxygen-free CO oxidation can be influenced by readsorption of  $\text{CO}_2$  formed,  $\text{CO}_2$  interaction with oxidized catalysts was also investigated. The flow of molecules in the single  $\text{CO}_2$  pulse experiments and the time were normalized in a dimensionless form according to [14]. The dimensionless flow is defined as  $F_A \cdot L^2 \cdot D^{-1} \cdot N_{p,A}$ , where  $F_A$  is the instantaneous flow (molecules  $\text{s}^{-1}$ ) of component A measured at the reactor outlet,  $L$  is the reactor length,  $D$  is the Knudsen diffusion coefficient of A, and  $N_{p,A}$  is the pulse size of A. The normalized transient response of inert gases is called the standard diffusion curve, and is used to discriminate between diffusion transport and chemical processes (e.g., adsorption, desorption, and reaction). Fig. 5 illustrates the normalized transients of Ne and  $\text{CO}_2$  after pulsing a  $\text{CO}_2/\text{Ne} = 1/1$  mixture over the catalysts at 573 K. For all the catalysts, the dimensionless flow of  $\text{CO}_2$  is first located within and then crosses the standard diffusion curve. According to [14], this is a fingerprint of reversible  $\text{CO}_2$  adsorption. Based on the intensity of the normalized  $\text{CO}_2$  flow and on the crossing point of the  $\text{CO}_2$  transients with that of Ne, it can be concluded that Pt/CZ-D and Pt/CZ-O adsorb  $\text{CO}_2$  strongly, but desorb it slowly. This is not the case for Pt/CZ-R. The difference between the catalysts can be explained as follows. In contrast to Pt/CZ-R, the apparent Pt surface density over Pt/CZ-D, and Pt/CZ-O is very low (Table 1). This means that a large portion of bare support ( $\text{CeO}_2\text{--ZrO}_2$ ) over these catalysts is exposed to the gas phase. Due to the basic nature of  $\text{CeO}_2$ ,  $\text{CO}_2$  adsorption occurs preferably over  $\text{CeO}_2$ , while  $\text{ZrO}_2$  can only weakly adsorb CO and/or  $\text{CO}_2$  [22]. Since the BET surface area of Pt/CZ-R is very low and the Pt surface density is high, it is expected that bare support is mainly covered by Pt particles reducing  $\text{CO}_2$  adsorption over the support. Thus, it is suggested that the strong  $\text{CO}_2$  adsorption over the bare support is a reason for the low- $\text{CO}_2$  formation in oxygen-free CO oxidation over Pt/CZ-D and Pt/CZ-O.

As demonstrated in [23,24], useful kinetic information can be derived from simple analysis of the position of ( $t_{\text{max}}$ ) of the maximal concentration of feed components and reaction products. Therefore, we analyze now the  $t_{\text{max}}$  values of  $\text{CO}_2$ . It is very important to emphasize that the  $\text{CO}_2$   $t_{\text{max}}$  in the  $\text{CO}_2$  pulse experiments is independent of the catalyst composition despite significant differences in the  $\text{CO}_2$  adsorption. Since the strong adsorption of  $\text{CO}_2$  does not result in an increase in the  $t_{\text{max}}$  value (Fig. 6), the  $t_{\text{max}}$  values of  $\text{CO}_2$  in the CO pulse experiments can be considered as an indicator of the intrinsic rate of  $\text{CO}_2$  formation (oxygen release speed); the smaller the  $t_{\text{max}}$  value, higher should be the rate of  $\text{CO}_2$  formation. It should be specially mentioned that such an analysis is possible only when mass transport via diffusion is not influenced by the catalyst composition, as confirmed in the present study. Otherwise, the difference between the  $t_{\text{max}}$  values of  $\text{CO}_2$  and inert gas pulsed together with  $\text{CO}_2$  should be considered. Fig. 6 compares the  $t_{\text{max}}$  values of  $\text{CO}_2$  transients in the oxygen-free CO pulse experiments. It should be noted that  $t_{\text{max}}$  was determined from the first  $\text{CO}_2$  pulse in the CO multi-pulse experiment. This is an important experimental restriction because CO is oxidized to  $\text{CO}_2$  over fully oxidized catalysts. Therefore, any influence of the reduction degree of the catalysts on  $\text{CO}_2$  formation and/or  $\text{CO}_2$  reduction can be excluded with increasing numbers of CO pulses. For all the catalysts, the  $t_{\text{max}}$  decreases with an increase in temperature. This means that  $\text{CO}_2$  formation is accelerated by temperature. With respect to the  $\text{CO}_2$   $t_{\text{max}}$  values at 523 K, the studied catalysts can be ordered as follows: Pt/CZ-D < Pt/CZ-O < Pt/CZ-R. This means that the rate for CO oxidation to  $\text{CO}_2$  at 523 K is the lowest over Pt/CZ-R. However, the catalysts do not differ significantly in the  $t_{\text{max}}$  values, when CO was pulsed at 623 K. In other words, the rate of  $\text{CO}_2$  formation increases more rapidly with temperature over the Pt/CZ-R material than over Pt/CZ-O and

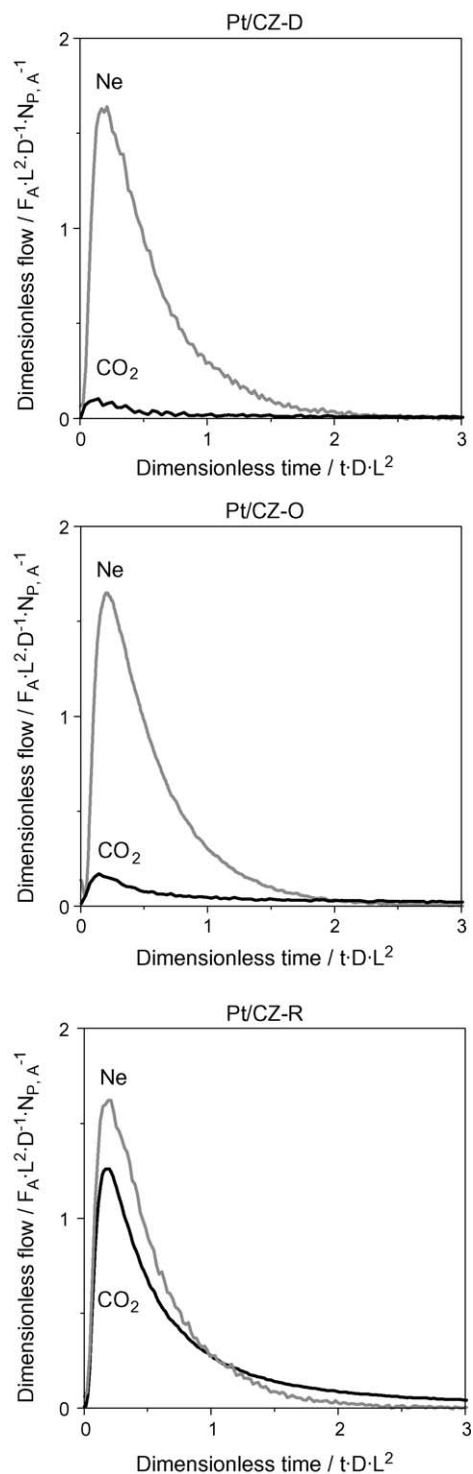
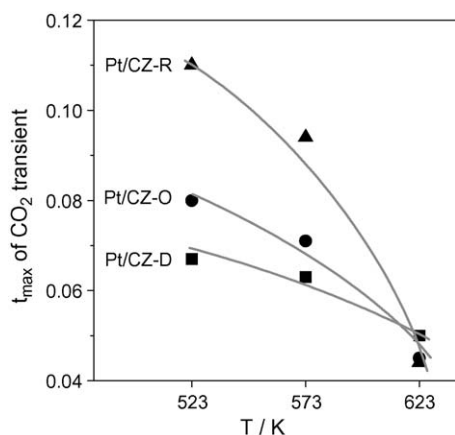


Fig. 5. Dimensionless  $\text{CO}_2$ , Ne transients after pulsing  $\text{CO}_2/\text{Ne} = 1/1$  over Pt/CZ-D, Pt/CZ-O, and Pt/CZ-R at 573 K. Pulse size of  $\text{CO}_2$  is ca.  $2 \times 10^{14}$ .

Pt/CZ-D. This agrees well with the results of CO and  $\text{O}_2$  cyclic experiments shown in Fig. 2 and with the temperature dependence of the initial rate for oxygen release as determined in [9].

In order to determine whether the high performance of Pt/CZ-R in oxygen-free CO oxidation to  $\text{CO}_2$  changes with increasing CO pulses, individual (non-average)  $\text{CO}_2$  responses detected in the 1st, 6th, 9th, 10th, 15th, 30th, 60th, and 90th CO pulses were analyzed. Since the CO pulse size in the TAP reactor was ca. 50 times lower than the total amount of surface oxygen species and CO conversion was almost complete, the  $\text{CO}_2$  responses in these CO pulses should



**Fig. 6.** Time ( $t_{\max}$ ) of maximum of  $\text{CO}_2$  transient responses after CO ( $\text{CO}/\text{Ne} = 1/1$ ) pulsing over Pt/CZ-D, Pt/CZ-O, and Pt/CZ-R at different temperatures.

reflect the effect of the degree of catalyst reduction on  $\text{CO}_2$  production. Fig. 7 exemplifies individual  $\text{CO}_2$  responses detected at 523 and 623 K. The intensity and the shape of  $\text{CO}_2$  transient responses change with an increase in the amount of CO pulsed at 523 K. The highest  $\text{CO}_2$  production was observed in the first CO pulse, which then decreased with an increase in the amount of pulsed CO. Simultaneously, the  $\text{CO}_2$  responses became broader. It is also important to highlight that the  $\text{CO}_2$   $t_{\max}$  increases with the number of CO pulses, indicating a decrease in the rate of  $\text{CO}_2$  formation. This may be due to an increase in the strength of the Ce–O bond following an increase in the reduction degree of  $\text{CeO}_x$  species. On the other hand, no significant changes in the shape and  $t_{\max}$  of  $\text{CO}_2$  transients were observed at 623 K. This may be explained by the fact that diffusion of bulk oxygen species to the catalyst surface increases with temperature, resulting in the reoxidation of reduced surface sites. Therefore, the reduction

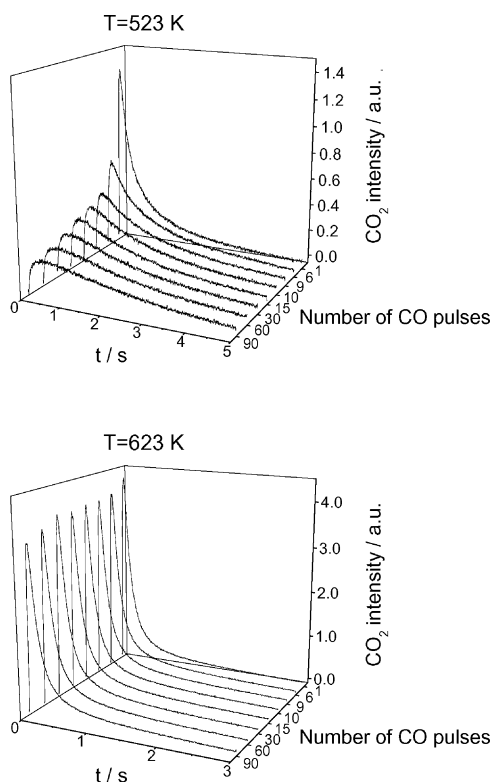


**Fig. 7.** Individual  $\text{CO}_2$  responses after CO ( $\text{CO}/\text{Ne} = 1/1$ ) pulsing over Pt/CZ-R at 523 and 623 K.

degree of the catalyst surface is not significantly changed at 623 K in contrast to 523 K. This suggestion is indirectly supported by the results of  $\text{O}_2$  and CO sequential pulse experiments in the next section.

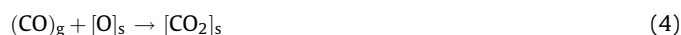
### 3.3. Reactivity of oxygen species for CO oxidation

The effect of gas-phase  $\text{O}_2$  on CO oxidation to  $\text{CO}_2$  was investigated by means of sequential pulsing of  $\text{O}_2/\text{Xe} = 1/1$  and  $\text{CO}/\text{Ne} = 1/1$  as well as  $\text{CO}/\text{Ne} = 1/1$  and  $\text{O}_2/\text{Xe} = 1/1$  mixtures with a time delay of 0.1 s between the pulses. The latter experiment can be considered as sequential pulses of  $\text{O}_2/\text{Xe} = 1/1$  and  $\text{CO}/\text{Ne} = 1/1$  with a time delay of 5.9 s between the  $\text{O}_2$  and CO pulses, since the  $\text{CO}/\text{Ne} = 1/1$  and  $\text{O}_2/\text{Xe} = 1/1$  sequence was repeated every 6 s. The application of two strongly differing time delays (0.1 and 5.9 s) between the  $\text{O}_2$  and CO pulses is essential for analyzing the effect of the lifetime of adsorbed oxygen species on their reactivity for CO oxidation to  $\text{CO}_2$ . In addition, the  $\text{CO}/\text{Ne} = 1/1$  and  $\text{O}_2/\text{Xe} = 1/1$  sequence is important in investigating whether adsorbed CO-containing surface species can be oxidized to  $\text{CO}_2$  in the presence of gas-phase  $\text{O}_2$ . Fig. 8 shows the transient responses of  $\text{O}_2$ , CO, and  $\text{CO}_2$  upon sequential pulsing of  $\text{O}_2$  and CO as well as of CO and  $\text{O}_2$ . Regardless of the order of pulsing of  $\text{O}_2$  and CO,  $\text{CO}_2$  was formed in the CO pulse. Moreover,  $\text{CO}_2$  concentration does not depend on the time delay between the  $\text{O}_2$  and CO pulses, indicating that lattice oxygen is responsible for CO oxidation to  $\text{CO}_2$  rather than short-lived adsorbed (non-lattice oxygen) oxygen species. As in CO multi-pulse experiments, traces of  $\text{CO}_2$  were detected in the sequential pulse experiments over Pt/CZ-D and Pt/CZ-O, together with high consumption of CO, while Pt/CZ-R was highly active for  $\text{CO}_2$  formation. Therefore, it can be suggested that the presence of oxygen is not a crucial requirement for  $\text{CO}_2$  formation over Pt/CZ-D and Pt/CZ-O, but may be the strong  $\text{CO}_2$  adsorption (Section 3.3).

Another important result is the effect of  $\text{O}_2$  on the shapes and the  $t_{\max}$  values of  $\text{CO}_2$  transients detected in the CO pulse. In contrast to oxygen-free CO oxidation to  $\text{CO}_2$  at 523 K (Fig. 7), no changes in the  $t_{\max}$  values of  $\text{CO}_2$  transient responses were observed with an increase in the number of CO pulses in the  $\text{O}_2$  and CO sequential pulse experiments. This means that the rate of  $\text{CO}_2$  formation does not depend on the number of CO pulses. The stable  $\text{CO}_2$  production in these experiments can be explained as follows. In the CO pulse, lattice oxygen is removed from the catalysts as  $\text{CO}_2$  yielding reduced sites, which are reoxidized in the  $\text{O}_2$  pulse resulting in the formation of active sites for CO oxidation. Considering the results of oxygen-free CO oxidation to  $\text{CO}_2$  and the sequential pulse experiments, it can be concluded that the degree of catalyst reduction influences the catalyst activity in oxidation of CO to  $\text{CO}_2$  and can be easily tuned even at 523 K by periodical feeding of small amounts of gas-phase oxygen.

### 3.4. Mechanistic scheme of OSC

The results of present transient studies as well as of previous catalyst characterization [9,13] are discussed together in order to elaborate structure–activity relationships in OSC over Pt(1 wt%)/ $\text{CeO}_2$ – $\text{ZrO}_2$  materials possessing differently structured  $\text{CeO}_2$ – $\text{ZrO}_2$  supports and Pt particles with different apparent surface densities. Based on the results of our transient experiments and the literature [13,16–20], a simplified mechanistic scheme is introduced in Eqs. (4)–(13):



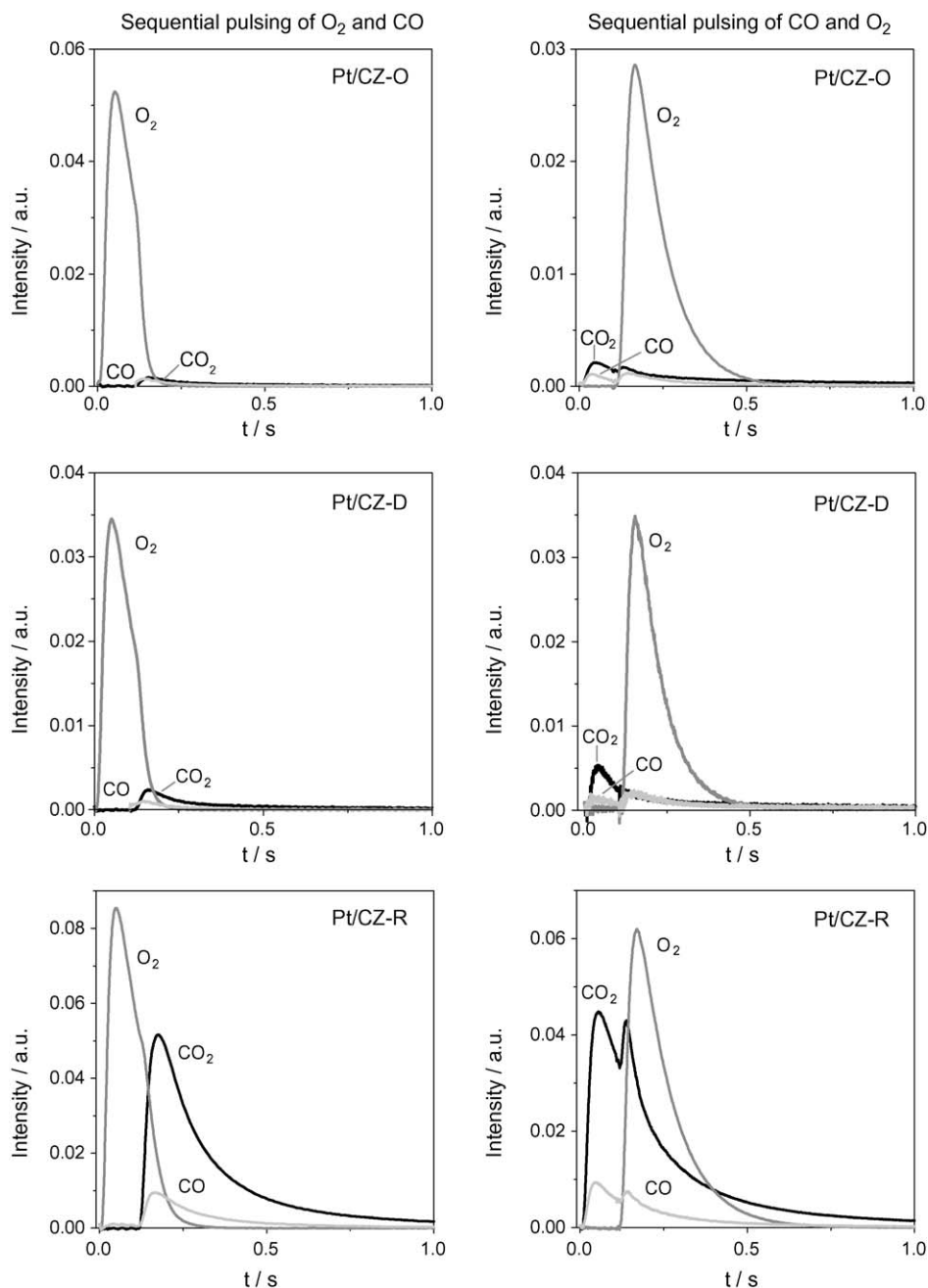
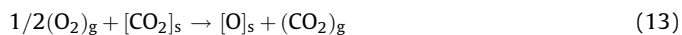


**Fig. 8.** Average transient responses of O<sub>2</sub>, CO, and CO<sub>2</sub> over Pt/CZ-R after sequential pulsing of O<sub>2</sub>/Xe = 1/1 and CO/Ne = 1/1 as well as CO/Ne = 1/1 and O<sub>2</sub>/Xe = 1/1 mixtures with  $\Delta t$  of 0.1 s at 573 K.



where [O] and [ ] are lattice oxygen and anion vacancy, respectively. Subscripts g, s, and b indicate for gaseous, surface, and bulk species, respectively.

In agreement with previous studies on CO oxidation over Pt-containing catalysts [12,25] and CeO<sub>2</sub>–ZrO<sub>2</sub> materials [16,17,20], gas-phase CO is activated over surface oxygen species yielding an adsorbed CO<sub>2</sub> species (Eq. (4)). In the presence of Pt on the catalyst surface, adsorption of gas-phase O<sub>2</sub> over reduced Ce-sites (Eq. (11)) causes significant backspillover of oxygen from CeO<sub>2</sub>–ZrO<sub>2</sub> support materials to the Pt surface, where CO oxidation occurs. The adsorbed CO<sub>2</sub> species decomposes, resulting in gas-phase CO<sub>2</sub> and reduced surface site (Eq. (5)). The adsorbed CO<sub>2</sub> can also be transformed to gas-phase CO<sub>2</sub> via its reaction with gas-phase O<sub>2</sub> (Eq. (13)). As suggested in [13,26], diffusion of lattice oxygen through the catalysts to the surface is also responsible for the reoxidation of reduced surface sites (Eq. (12)). This reaction

pathway can be tuned by the method for the preparation of CeO<sub>2</sub>–ZrO<sub>2</sub> support materials [9]. Oxygen mobility within the support is increased when Zr ions are distributed in CeO<sub>2</sub> as homogeneously as possible [13]. Besides the above processes responsible for OSC, several side reactions influence the OSC performance. As shown in Section 3.3, gas-phase CO<sub>2</sub> strongly adsorbs over oxidized catalytic materials blocking active sites ([O]) for CO oxidation to CO<sub>2</sub> (Eq. (6)); thus, diminishing the OSC performance. Furthermore, not only active oxidized sites but also reduced surface sites can be occupied by CO<sub>2</sub> (Eq. (8)). In this case, the OSC performance will also decrease, because the reaction pathway in Eq. (11) cannot contribute to the reoxidation of surface reduced sites due to their blockage by adsorbed CO<sub>2</sub>. The CO<sub>2</sub> adsorbed over reduced ceria can desorb (Eq. (9)) or reoxidize the catalyst yielding gas-phase CO (Eq. (10)). The latter reaction is accelerated by temperature and by addition of ZrO<sub>2</sub> to CeO<sub>2</sub> [27–29]. The strong adsorption of CO<sub>2</sub> can be suppressed when basic CeO<sub>2</sub> is covered either by active Pt particles or by acid promoters, which do not inhibit redox properties of CeO<sub>2</sub>. Kakuta et al. [30] have shown that promoting CeO<sub>2</sub>–ZrO<sub>2</sub> with MgO did not significantly influence the redox performance, but prevented deterioration of OSC performance by the sintering.

Thus, for achieving high-OSC performance, it is important to design catalytic surfaces that readily provide lattice oxygen for CO oxidation directly yielding gas-phase CO<sub>2</sub> and reduced surface sites. The latter should be quickly reoxidized by bulk lattice oxygen via its diffusion to the catalyst surface. Moreover, CO<sub>2</sub> adsorption over oxidized and reduced sites should be very weak in order to minimize the poisoning of surface oxidized and reduced sites participating in reduction and oxidation reactions of OSC.

Finally, we discuss the method for correct evaluation of the oxygen release speed from OSC catalyst. When we analyze OSC using CO and O<sub>2</sub> as probe molecules, CO, O<sub>2</sub>, and CO<sub>2</sub> are quantitatively determined in the gas phase. It would be expected that the amount of CO<sub>2</sub> detected in the gas phase upon oxygen-free CO oxidation represents correctly the OSC and the oxygen release speed. Our mechanistic analysis of CO<sub>2</sub> adsorption suggested that the strong adsorption of CO<sub>2</sub> over bare support material influences OSC measurements at ambient pressure and even in high vacuum when powdered catalysts are used. The CO<sub>2</sub> readsorption in the CO pulse experiments in the TAP reactor could not be excluded by reducing the height of the catalyst bed to 0.3 mm. Therefore, it is difficult to evaluate the oxygen release speed from the amount of CO<sub>2</sub> formed. The present study concludes that the position ( $t_{\max}$ ) of the maximal concentration of CO<sub>2</sub> in oxygen-free CO pulse experiments in the TAP reactor is a representative indicator for the oxygen release speed; the lower the  $t_{\max}$  value, higher is the speed. Alternatively, for proper determination of the OSC performance, experiments should be performed in vacuum using flat catalysts [12], because CO<sub>2</sub> formed is directly emitted to vacuum without returning to the catalyst. Tanabe et al. [9] have also showed that the effect of CO<sub>2</sub> readsorption on the evaluation of the OSC can be minimized by performing tests with high-gas flows (5 l min<sup>−1</sup> per 1.0 g catalyst).

#### 4. Conclusions

Transient studies on oxygen-free CO oxidation over three Pt(1 wt%)/ZrO<sub>2</sub>–CeO<sub>2</sub> materials established that the catalyst ability

for oxygen storage capacity (OSC) defined as the ratio of the amount of CO<sub>2</sub> produced to the overall amount of Ce atoms depends strongly on the surface distribution of Pt particles and the homogeneity of the distribution of Zr in the lattice of CeO<sub>2</sub>. Pt particles with large surface areas (low dispersion) and Zr distribution as homogeneous as possible are key factors governing the OSC performance.

For correct determination of the OSC performance, it is highly important to perform experiments under such conditions where readsorption of CO<sub>2</sub> formed from CO is minimized. Otherwise, CO<sub>2</sub> adsorbs strongly over bare supports (not covered by Pt particles), and the amount of CO<sub>2</sub> detected in the gas phase incorrectly represents the catalyst's CO-oxidation ability. One approach is to perform simple CO pulse experiments in the TAP reactor operating in vacuum. Although CO<sub>2</sub> adsorption cannot be completely avoided, we found that the O<sub>2</sub> release speed and the OSC are correctly determined from the analysis of the position ( $t_{\max}$ ) of the maximal CO<sub>2</sub> concentration in the CO<sub>2</sub> transient detected upon oxygen-free CO oxidation. Moreover, this analysis enables us to determine whether the O<sub>2</sub> release speed is influenced by the reduction degree of the catalysts.

#### References

- [1] S. Matsumoto, N. Miyoshi, T. Kanazawa, M. Kimura, M. Ozawa, in: S. Yoshida, T.N. Tabezawa, T. Ono (Eds.), *Catalytic Science and Technology*, vol.1, Kodansha-VCH, Tokyo, 1991, p. 335.
- [2] S. Matsumoto, H. Shinjoh, *Adv. Chem. Eng.* 33 (2007) 1.
- [3] A. Trovarelli, F. Zamar, J. Llorca, C. de Leitenburg, G. Dolcetti, J.T. Kiss, *J. Catal.* 169 (1997) 490.
- [4] A. Holmgren, B. Andersson, D. Duprez, *Appl. Catal. B* 22 (1999) 215.
- [5] C.E. Hori, A. Brenner, K.Y. Simon Ng, K.M. Rahmoeller, D. Belton, *Catal. Today* 50 (1999) 299.
- [6] M. Boaro, C. de Leitenburg, G. Dolcetti, A. Trovarelli, *J. Catal.* 193 (2000) 338.
- [7] H. Vidal, J. Kaspar, M. Pijolat, G. Colon, S. Bernal, A. Cordón, V. Perrichon, F. Fally, *Appl. Catal. B* 27 (2000) 49.
- [8] S. Bedrane, C. Descorme, D. Duprez, *Stud. Surf. Sci. Catal.* 138 (2001) 125.
- [9] T. Tanabe, A. Suda, C. Descorme, D. Duprez, H. Shinjoh, M. Sugiura, *Stud. Surf. Sci. Catal.* 138 (2001) 135.
- [10] H. Vidal, J. Kaspar, M. Pijolat, G. Colon, S. Bernal, A. Cordón, V. Perrichon, F. Fally, *Appl. Catal. B* 30 (2001) 75.
- [11] J. Fan, X. Wu, X. Wu, Q. Liang, R. Ran, D. Weng, *Appl. Catal. B* 81 (2008) 38.
- [12] Y. Sakamoto, K. Kizaki, T. Motohiro, Y. Yokota, H. Sobukawa, M. Uenishi, H. Tanaka, M. Sugiura, *J. Catal.* 211 (2002) 157.
- [13] F. Dong, A. Suda, T. Tanabe, Y. Nagai, H. Sobukawa, H. Shinjoh, M. Sugiura, C. Descorme, D. Duprez, *Catal. Today* 93–95 (2004) 827.
- [14] J.T. Gleaves, G.S. Yablonskii, P. Phanawadee, Y. Schuurman, *Appl. Catal. A* 160 (1997) 55.
- [15] J. Pérez-Ramírez, E.V. Kondratenko, *Catal. Today* 121 (2007) 160.
- [16] M. Boaro, F. Giordano, S. Recchia, V.D. Santo, M. Giona, A. Trovarelli, *Appl. Catal. B* 52 (2004) 225.
- [17] C. Descorme, R. Taha, N. Mouaddib-Moral, D. Duprez, *Appl. Catal. A* 223 (2002) 287.
- [18] N. Hickey, P. Fornasiero, J. Kaspar, J.M. Gatica, S. Bernal, *J. Catal.* 200 (2001) 181.
- [19] S. Hilaire, X. Wang, T. Luo, R.J. Gorte, J. Wagner, *Appl. Catal. A* 215 (2001) 271.
- [20] M. Zhao, M. Shen, J. Wang, *J. Catal.* 248 (2007) 258.
- [21] Y. Madier, C. Descorme, A.M. Le Govic, D. Duprez, *J. Phys. Chem.* 103 (1999) 10999.
- [22] C. Monterra, G. Cerrato, F. Pinna, *Spectrochim. Acta A* 55 (1995) 95.
- [23] J. Pérez-Ramírez, E.V. Kondratenko, *J. Catal.* 250 (2007) 240.
- [24] E.V. Kondratenko, V.A. Kondratenko, M. Santiago, J. Pérez-Ramírez, *J. Catal.* 256 (2008) 248.
- [25] S.O. Shekhtman, A. Goguet, R. Burch, C. Hardacre, N. Maguire, *J. Catal.* 253 (2008) 303.
- [26] F. Dong, T. Tanabe, A. Suda, N. Takahashi, H. Sobukawa, H. Shinjoh, *Chem. Eng. Sci.* 63 (2008) 5020.
- [27] K. Otsuka, T. Ushiyama, I. Yamanaka, *Chem. Lett.* (1993) 1517.
- [28] K. Otsuka, Y. Wang, E. Sunada, I. Yamanaka, *J. Catal.* 175 (1998) 152.
- [29] K. Otsuka, Y. Wang, M. Nakamura, *Appl. Catal. A* 183 (1999) 317.
- [30] N. Kakuta, Y. Kudo, T. Eguchi, H. Ohkita, T. Mizushima, T. Yamamoto, M. Yasuda, *Stud. Surf. Sci. Catal.* 162 (2006) 777.